



HAL
open science

Ultrafast electron energy-dependent delocalization dynamics in germanium selenide

Zhesheng Chen, Heqi Xiong, Hao Zhang, Chaofeng Gao, Yingchun Cheng,
Evangelos Papalazarou, Luca Perfetti, Marino Marsi, Jean-Pascal Rueff

► **To cite this version:**

Zhesheng Chen, Heqi Xiong, Hao Zhang, Chaofeng Gao, Yingchun Cheng, et al.. Ultrafast electron energy-dependent delocalization dynamics in germanium selenide. *Communications Physics*, 2021, 4, pp.138. <10.1038/s42005-021-00635-y>. <hal-03272214>

HAL Id: hal-03272214

<https://hal.sorbonne-universite.fr/hal-03272214v1>

Submitted on 28 Jun 2021

HAL is a multi-disciplinary open access archive for the deposit and dissemination of scientific research documents, whether they are published or not. The documents may come from teaching and research institutions in France or abroad, or from public or private research centers.

L'archive ouverte pluridisciplinaire **HAL**, est destinée au dépôt et à la diffusion de documents scientifiques de niveau recherche, publiés ou non, émanant des établissements d'enseignement et de recherche français ou étrangers, des laboratoires publics ou privés.



HAL Authorization

Ultrafast electron energy-dependent delocalization dynamics in germanium selenide

Zhesheng Chen^{1,2,3✉}, Heqi Xiong⁴, Hao Zhang⁴, Chaofeng Gao⁴, Yingchun Cheng^{4✉}, Evangelos Papalazarou², Luca Perfetti³, Marino Marsi² & Jean-Pascal Rueff^{1,5✉}

Ultrafast scattering process of high-energy carriers plays a key role in the performance of electronics and optoelectronics, and have been studied in several semiconductors. Core-hole clock spectroscopy is a unique technique for providing ultrafast charge transfer information with sub-femtosecond timescale. Here we demonstrate that germanium selenide (GeSe) semiconductor exhibits electronic states-dependent charge delocalization time by resonant photo exciting the core electrons to different final states using hard-x-ray photoemission spectroscopy. Thanks to the experiment geometry and the different orbital polarizations in the conduction band, the delocalization time of electron in high energy electronic state probed from Se *1s* is ~470 as, which is three times longer than the delocalization time of electrons located in lower energy electronic state probed from Ge *1s*. Our demonstration in GeSe offers an opportunity to precisely distinguish the energy-dependent dynamics in layered semiconductor, and will pave the way to design the ultrafast devices in the future.

¹Synchrotron SOLEIL, L'Orme des Merisiers, Gif-sur-Yvette, France. ²Laboratoire de Physique des Solides, CNRS, Université Paris Saclay, Orsay, France. ³Laboratoire des Solides Irradiés, Ecole Polytechnique, CNRS, CEA, Palaiseau, France. ⁴Key Laboratory of Flexible Electronics & Institute of Advanced Materials, Jiangsu National Synergetic Innovation Center for Advanced Materials, Nanjing Tech University, Nanjing, China. ⁵Laboratoire de Chimie Physique-Matière et Rayonnement, LCPMR, Sorbonne Université, CNRS, Paris, France. ✉email: zhesheng.chen@gmail.com; iameycheng@njtech.edu.cn; jean-pascal.rueff@synchrotron-soleil.fr

Ultrafast electron dynamics in semiconductors play a key role in the performance of electronics and optoelectronics, and it can be directly observed by pump-probe spectroscopies^{1–3}, such as time-resolved photoemission spectroscopy. In pump process, valence electrons are excited to the conduction band by a pump pulsed laser, and then they are ionized with another pulse with enough energy to probe the unoccupied electronic structure. In such a case, the dynamics of photoexcited states can be monitored^{4,5} by varying the pump-probe delay. However, the time resolution of pump-probe spectroscopy is dependent both on the time resolution of the laser itself and the whole spectroscopy setup, which is limited to femtosecond. In addition, the energy level of the final state in pump-probe spectroscopy is limited by pump energy, which is not a suitable way to study the electron dynamics in a semiconductor with band gap larger than the pump beam energy, as well as electron dynamics in very high electronic states. In recent years, the core-hole clock (CHC) spectroscopy has provided dynamics information as fast as tens of attoseconds^{6–11}, thus appearing as an ultrafast, complementary approach to pump-probe spectroscopy. This method uses an intrinsic timescale due to the core-hole lifetime of a specific atomic level, which allows us to elucidate electron–electron correlation effects and their role in excited electron dynamics. It has been widely used in the ultrafast charge transfer determination between the interfaces, such as absorbed molecules and substrates. Generally, the faster of charge transfer, the higher transport properties of the electronic devices due to efficient electron decoupling from atoms and less carrier recombination. Föhlisch et al. showed that the charge transfer from an adsorbed sulfur atom to a ruthenium surface proceeds in ~ 320 as⁸. Moreover, CHC method can also distinguish the photoexcited electron delocalization time in layered materials. For example, in layered SnS₂ semiconductor, Eads et al. found spin-dependent attosecond charge delocalization time, which is ~ 400 as within intralayer, while >2.7 fs between interlayers¹². In addition, Johansson et al. also observed the anisotropy in the x-ray absorption cross section in polarization direction in plane and out of plane of the SnS₂ crystal, by using CHC spectroscopy¹³. However, to the best of our knowledge, most of the previous work are focused on the carrier dynamics in fixed unoccupied states by resonant x-ray excitation, and it is still unclear the carrier dynamics behavior between different unoccupied states mainly due to the difficulty of finding a suitable system, which is very important for carrier dissipation and transport properties in electronic and optoelectronic devices.

Phosphorene-like structured two-dimensional materials, such as IV–VI (V = Ge, Sn; VI = S, Se) semiconductors have attracted strong interest due to their outstanding properties of high carrier mobility and planar anisotropy recently^{14–19}. The group of IV–VI compounds have advantages of unique orthorhombic structures and environmentally friendly features, which have opened up possibilities for various photonic and optoelectronic applications, such as polarization-dependent photodetectors and optical waveplates. Among these, the puckered lattice structure in germanium selenide (GeSe) gives rise to in-plane anisotropic response to external stimulations, such as polarized light illumination²⁰. GeSe has suitable band gap of 1.14 eV, high absorption coefficient of $>10^5$ cm⁻¹, and high carrier mobility of 128.6 cm⁻¹ V⁻¹ s⁻¹. The GeSe-based phototransistor has ultrahigh photoresponsivity of 1.6×10^5 AW⁻¹, which is two orders of magnitude higher than that of monolayer MoS₂ (ref. 21). From first-principle calculations, the thermoelectric figure of merit ZT in hole-doped monolayer GeSe is expected to be higher than that of other semiconductors, the experimentally confirmed material with the record value²².

Here, we performed the CHC experiment on layered GeSe semiconductor and investigated the electron dynamics in

different electronic states by using hard-x-ray resonant Auger spectroscopy at the Ge and Se *K*-edges. The delocalization timescales of electrons in conduction band probed from Ge 1s and Se 1s core levels are estimated at ~ 150 and ~ 470 as, respectively, which is three times different because of the different energy final states. Our findings demonstrate that CHC is a powerful method to study the electron energy-dependent dynamics. The state-dependent dynamics revealed in this study provides a unique handle to fine tune the ultrafast response of materials, offering an opportunity to design high performance ultrafast optoelectronic devices.

Results and discussion

Geometry of x-ray photoemission and electronic band structure of GeSe. GeSe compound has the similar layered structure compared to the elemental phosphorene single crystal. It contains double-layer slabs of Ge–Se in a chair configuration. There are two nonequivalent in-plane crystal directions armchair and zigzag, and the adjacent layers are stacked by weak van der Waals forces. GeSe has indirect band gap of ~ 1.1 eV with the valence band maximum and the conduction band minimum at different *k* points along armchair (Γ –*Y*) direction. The anisotropic properties of GeSe can be identified from the significant difference of band dispersions between armchair and zigzag (Γ –*X*) directions. All the sharp features from Raman spectrum and photoemission peaks of core levels indicate the high quality of our sample that grown by chemical vapor transport method (see Supplementary Note I for the Raman and x-ray photoemission spectra). CHC spectroscopy involves the resonant excitation of core electrons, which results in atomic and orbital specificities. For example, it can photoexcite the core electrons of a particular element of interest to the unoccupied states of specific symmetry selectively. The cross section for x-ray absorption that electrons are probed from core levels of Ge 1s or Se 1s can be approximated by the following equation²³:

$$\sigma = 4\pi^2 \hbar \omega \alpha \sum_f |\langle f | \hat{\epsilon} \cdot \mathbf{r} | \Phi_{1s} \rangle|^2 \delta(E_f - E_{1s} - \hbar\omega) \quad (1)$$

where $|\Phi_{1s}\rangle$ is core orbital of Ge 1s (or Ge 1s) and $|f\rangle$ is the corresponding unoccupied states of the system. The dipole operator $\hat{\epsilon} \cdot \mathbf{r}$ results in selection rules, which dictate the allowed change for the angular momentum quantum number (e.g., $\Delta l = \pm 1$ for dipolar transitions). It also imposes that the probed orbital must lie in the polarization plane. Figure 1a shows the experiment geometry of our x-ray photoemission experiment, including sample plane and *p* polarization of x-ray, which it can populate the specific orbital p_z in our case of an oriented sample. The band structure of GeSe is calculated from first-principles pseudopotential calculations that performed by using the projector augmented wave pseudopotentials implemented in the Vienna ab initio Simulation Package, and the GeSe band structure with Ge p_z and Se p_z orbitals are illustrated in Fig. 1b, c, respectively. We find very strong energy-dependent orbital contribution in GeSe, for example, the Ge p_z orbitals mainly distributes in the conduction bands and the density is very strong in the Γ –*Y* valley near to the conduction band minimum. In contrast, the Se p_z orbitals mainly distributes in the valence bands, and also the conduction bands that are 2–3 eV above the conduction band minimum. In this case, in x-ray absorption of our experiment, electrons from Ge 1s and Se 1s core levels can be resonantly excited to the corresponding final states $|f\rangle$ by *p*-polarized hard-x-ray, which is the Ge p_z orbital and Se p_z orbital contributed unoccupied states. In this case, the carrier dynamics in the two different final states can be compared separately, which also means GeSe semiconductor is an ideal system to study the energy-dependent dynamics by using CHC method. The other

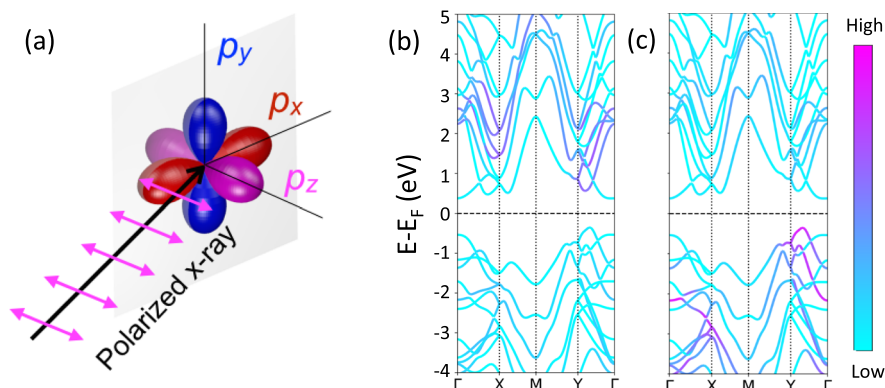


Fig. 1 Experimental geometry and orbital contributions. **a** The geometry of the sample and incident x-ray in our experiment; the horizontal polarized light (purple arrows) excites the p_z orbitals preferentially. **b** Calculated Ge p_z orbital contribution in GeSe band structure. **c** Calculated Se p_z orbital contribution in GeSe band structure. The colorbar indicates the weight of p_z contribution in the states.

calculated orbital contributions, such as Ge $p_{x,y}$ and Ge $p_{x,y}$ are shown in Supplementary Note II, and we cannot distinguish them because of our experiment geometry.

Core-hole clock spectroscopy in GeSe. The CHC method is briefly explained in the following. A core-hole (for example, Ge 1s or Se 1s) is created following the photoemission of a core electron by the incident x-rays. For the Auger process, an upper-level electron fills the core vacancy and another electron is emitted to the vacuum when a core-hole is formed, and the kinetic energy of the emitted electron contains information about the decay steps. The normal Auger decay generates a two-hole final states, as shown in Fig. 2a. However, two different phenomena may occur if the core-hole is created by a resonant excitation shown in Fig. 2b: on the one hand, the excited electron may recombine with the core-hole, causing a one-hole final state shown in Fig. 2c. On the other hand, the excited electrons can stay in the unoccupied state before recombining with the holes, leading to a two-hole and one electron final state shown in Fig. 2d. The two different relaxation processes are called participator and spectator, respectively. Furthermore, the photoexcited electron can be further transferred into bulk (delocalization) or substrate (charge transfer), if the transfer time is faster than the core-hole lifetime, as shown in Fig. 2e. Normally, the participator enhances the photoemission line of the resonant Auger spectra, while the spectator shifts kinetic energies slightly compared to normal Auger feature because of the screening of the spectator electron on the two core-holes. Moreover, the kinetic energy of the spectator Auger varies proportionally as a function of the photon energy. The time resolution of the CHC is limited by the lifetime of the core-hole, and normally lies within roughly one order of magnitude deviation from the core-hole lifetime. The p -polarized x-ray can excite core electrons from Ge 1s and Se 1s to different conduction bands according to the Ge p_z and Se p_z orbitals distribution, which gives us an opportunity to study the energy-dependent electron dynamics in GeSe.

X-ray absorption near-edge spectra (XANES). We firstly studied the x-ray absorption of Ge K -edge and Se K -edge in GeSe single crystal by using hard-x-ray photoemission spectroscopy (HAXPES). HAXPES has advantage of probing depth of the electrons up to tens of nm, which is a true bulk-sensitive probe compared to the soft-x-ray photoemission. In addition, since a deep, short-live, core-hole is created, HAXPES can probe ultra-fast dynamics well within the attosecond regime. As shown in Fig. 3a the XANES of Ge K is recorded from sample current, which is proportional to the emitted electron numbers. At the

edge, it contains the resonant excitation information that the electrons are photoexcited from the Ge 1s to the unoccupied bands built up from Ge $4p_z$ orbitals according to the excitation geometry. In addition, the XANES spectrum of Se K shows the similar feature that corresponds to the resonant excitation from Se 1s to the unoccupied bands built up from Se $4p_z$ orbitals as seen from Fig. 3c. The experiment absorption spectra are in good agreement with the simulations. Furthermore, we calculated the density of states (DOS) in GeSe, and the orbital contributions of Ge p_z and Se p_z in DOS are shown in Fig. 3b, d. It is worth noticing that the DOS used in the calculations includes the core-hole effect that is indicated in the figures. According to the DOS calculation, the states with main contribution of Ge p_z in conduction bands are close to Fermi level, while the states with main contribution of Se p_z in conduction bands is 2 eV above the Fermi level, which are in excellent agreement with the orbital distribution in GeSe band structure shown in Fig. 1b, c. Therefore, the final states of resonant photoemission from Ge 1s and Se 1s locate at different energy regions. The XAS simulations demonstrate that the absorption spectrum reflects the DOS of the atom of the same nature, meaning a Ge (resp. Se) 1s electron will be promoted to Ge (resp. Se) p_z orbital. Nonlocal dipolar transitions from Ge to Se (and vice versa) are not favored and can be considered as negligible.

Resonant Auger photoemission spectra. The resonant photoemission maps of Auger emission intensity as functions of photon excitation energy and photoelectron kinetic energy are shown in Fig. 4. The intensity map in Fig. 4a shows a strong resonant enhancement of the Ge KLL ($1s2p_{1/2}2p_{3/2}$) Auger features when the photon energy is scanned across the Ge K -edge. The dominant transition in the Ge KLL normal Auger spectrum is the transition at electron kinetic energies of 8.562 keV accompanied with several weaker structures at 8 eV lower kinetic energy. The coherent normal Auger feature and dispersing in-coherent feature of spectator are clearly observed. The delocalization time τ_{deloc} of resonant photoexcited electron in the p_z orbital states of conduction band can be obtained directly from the ratio of the integrated spectral components:

$$\tau_{\text{deloc}} = (I_{\text{SA}}/I_{\text{NA}}) \times \tau_{1s} \quad (2)$$

where τ_{1s} is the core-hole lifetime of Ge 1s, I_{SA} and I_{NA} are the intensities of the spectator and normal Auger component, respectively. The lifetime of the core-hole is reflected in a Lorentzian broadening of the spectral profile. The Ge 1s x-ray photoelectron spectrum was taken at photon energy of 11.5 keV, far above the ionization threshold. The lifetime of τ_{1s} can be obtained

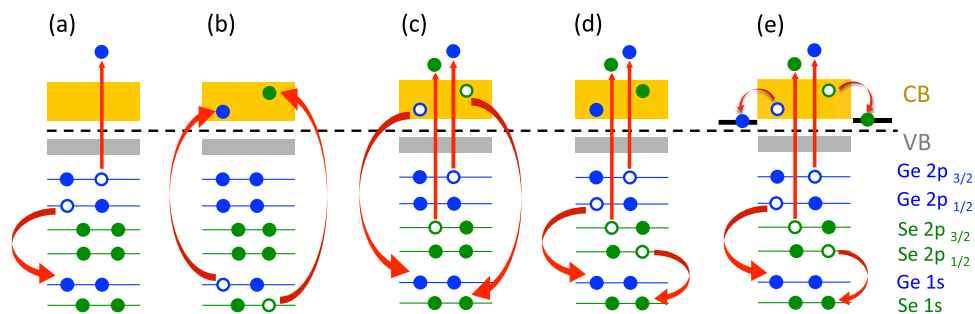


Fig. 2 Schematic overview of working principle of the core-hole clock spectroscopy. **a** Normal Auger process. **b** Resonant photoexcitation from core level to conduction band. **c** Participator decay process. **d** Spectator decay process. **e** Charge delocalization or charge transfer process. CB and VB indicate conduction band and valence band, blue solid circles and hollow circles indicate electrons and holes from Ge core levels, and green solid circles and hollow circles indicate electrons and holes from Se core levels, respectively.

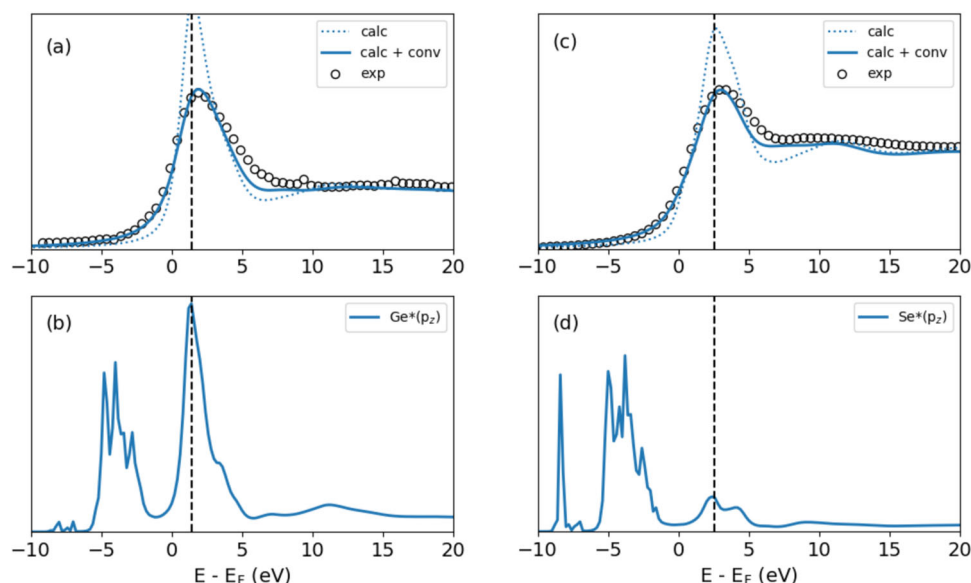


Fig. 3 X-ray absorption: experimental results and theory calculation. **a** XANES and the calculated x-ray absorption spectra of Ge K. **b** Calculated density of states with orbital contributions of Ge p_z . **c** XANES and the calculated x-ray absorption spectra of Se K. **d** Calculated density of states with orbital contributions of Se p_z . The open circles in **a** and **c** are experimental data, and the lines are the calculated data. In all the plots, we use a relative energy scale with respect to the Fermi energy E_F . To ease the comparison with the experimental data (hollow circle line), the calculated XANES spectra (dotted line) were convolved with a Lorentzian profile, resulting in broadened spectra (solid line). The black dashed lines in **b** and **d** indicate the positions of maximum p_z orbital contributions in the unoccupied states.

by:

$$\tau_{1s} = \hbar/W \quad (3)$$

where W is the full-width at half-maximum of the core-level spectrum. The lifetime of Ge 1s core-hole is estimated at 0.32 fs from the full-width at half-maximum of the 1s core-level photoemission spectrum. In the following, the normal Auger spectrum taken at photon energy of 11.123 keV was fitted above the ionization threshold, in order to get a fixed energy position for the main peak, as shown in Fig. 4c. Figure 4d shows the maximum resonance excitation Auger spectrum taken at the photon energy of 11.111 keV, which corresponds to the photon energy at maximum x-ray absorption in XANES curve of Fig. 3a. The spectrum can be fitted very well by normal Auger peak and spectator Auger peak, and the electron delocalization time τ_{deloc} of electron from Ge KLL can be calculated from equation, which is ~ 150 as. We also analyzed the delocalization time τ_{deloc} of Se KLL according to the resonant Auger map in Fig. 4b, and the corresponding normal Auger spectrum taken at photon energy of 12.678 keV in Fig. 4e, as well as the maximum resonance excitation Auger spectrum taken at photon energy of 12.665 keV in Fig. 4f. The lifetime of Se

1s core-hole is estimated at ~ 0.30 fs, which is almost the same compared to that of Ge 1s, while the delocalization time τ_{deloc} of electron from Se KLL is estimated at ~ 470 as, which is three times longer than that of Ge KLL . We recall that the resonant photoexcitation of Ge 1s and Se 1s have ~ 2 eV energy difference, as shown in the p_z peak in the DOS of Fig. 3c, d, thus we attribute the significant difference of delocalization time to the final states with different energy levels. The differential carrier dynamics as a function of final states have been also observed from pump-probe spectroscopy, for example, in our previous study, the final states of electrons that pumped by second harmonic pulse (3.12 eV) have access energy of >1 eV in InSe semiconductor, and the hot electrons can stay in the conduction band ~ 2 ps before cooling down to conduction band minimum, while the cooling time of hot electrons pumped by fundamental pulse (1.56 eV) is ~ 0.47 ps as the final states are very close to conduction band minimum²⁴. The ultrafast dynamics that we extracted from CHC spectroscopy is relevant to the performance of electronic devices. As the excitation by x-ray is localized on a specific site due to the creation of a core-hole, the timescale measured by CHC method reflects the decoupling time of an excited electron from a specific

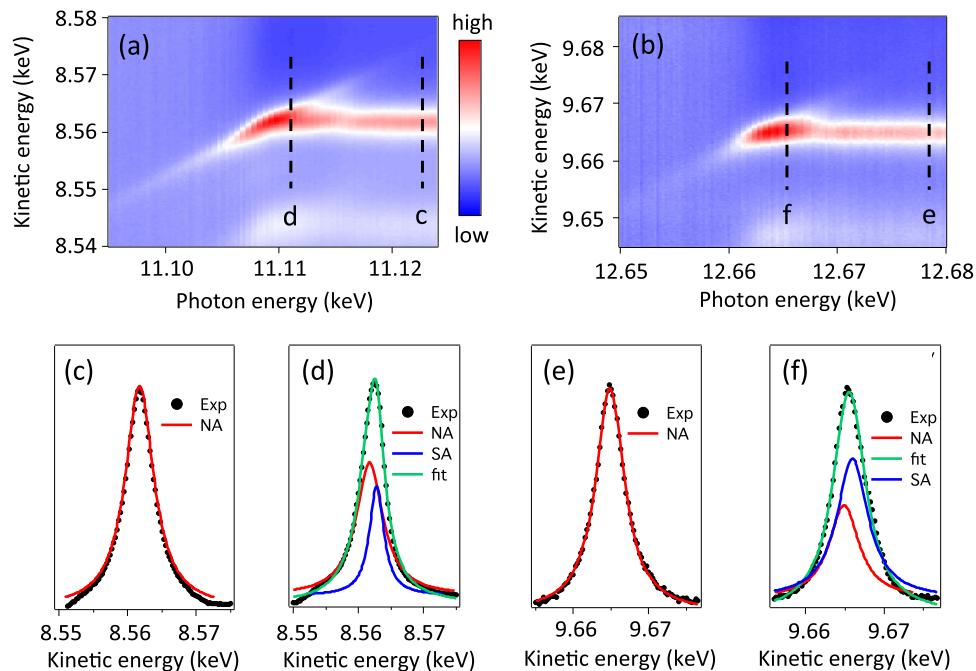


Fig. 4 Resonant Auger photoemission spectra. **a** Resonant Auger maps of Ge *KLL*. **b** Resonant Auger maps of Se *KLL*. **c, d** Resonant photoemission spectra of Ge *KLL* are recorded at the photon energy at 11.123 and 11.111 keV. **e, f** Resonant photoemission spectra of Se *KLL* are recorded at the photon energy at 12.678 and 12.665 keV. These excitation energies are indicated by dashed lines in **a** and **b**. The experimental spectra are shown in dotted black curves, and they are fitted by normal Auger peak (red curves) and spectator Auger peak (blue curves) in **c-f**.

atom, which gains information for the transport properties in real devices. The method can be also well adopted to study charge dynamics in spintronic devices. For example, in materials based on Mn perovskites, charge transfer between a Mn^{3+} ion and a Mn^{4+} ion via a double exchange mechanism involving oxygen atoms is the main reason for the colossal magnetoresistance effect, and such charge transfer dynamics can be determined from CHC technique⁶. However, it is worth emphasizing here again that the timescales measured by CHC are different from that of pump-probe spectroscopy. The difference arises from the fact that the exciton created by optical excitation between valence band and the conduction band is delocalized, and the timescale measured by pump-probe technique is the relaxation dynamics of hot carriers that corresponds to electron-phonon scattering process. On the other hand, the energy of final states from pump-probe technique is limited by the pump energy and the size of band gap, while it is dependent on the geometry and orbital contribution in CHC method. The localization property makes CHC spectroscopy chemically specific and the resonant Auger pathways are very sensitive to the local energy landscape of the excited electron. Therefore, we demonstrate that the CHC spectroscopy can be an efficient way to study the delocalization time of photoexcited electrons in different energy final states by selective x-ray excitation of core electrons into unoccupied states, which is a complementary method with pump-probe techniques.

Conclusions

In conclusion, we performed CHC measurement on bulk semiconductor GeSe by using HAXPES. Owing to the geometry of our experiment and the energy-dependent p_z orbital contribution of Ge and Se, we could resonant probe the electrons from core levels of Ge 1s and Se 1s to different final states, respectively. Our data show that the delocalization time of electron in higher energy final states from Ge *KLL* Auger spectra are three times longer than that of lower energy final states from Se *KLL* Auger spectra. Our observation demonstrate that the CHC spectroscopy is an efficient

way to investigate the electron delocalization dynamics in energy-dependent final states, and is a complementary method with pump-probe technique. The attosecond delocalization time determined in GeSe could advantageously serve to engineer ultrafast devices based on layered semiconductor heterostructures.

Methods

Sample and HAXPES experiment. High-quality single crystals of GeSe were grown by chemical vapor transport method²⁵. The clean surfaces of the samples were obtained by cleaving the sample in the preparation chamber under high vacuum of 5×10^{-8} mbar, and were transferred into experiment chamber immediately at the base pressure of 5×10^{-9} mbar. All the photoemission experiments were performed at the Synchrotron SOLEIL on the hard-x-ray photoelectron spectroscopy endstation of the GALAXIES beamline, which covers the 2.3–12 keV photon energy range and provides horizontal polarization^{26,27}. Electrons are analyzed by a large-acceptance-angle EW4000 SCIENTA hemispherical analyzer, with its lens axis set collinear to the x-ray polarization. The binding energy of the spectra was calibrated by measuring the Fermi edge of an Au film. The overall energy resolution was estimated to be ~ 0.25 eV from Fermi edge fitting. The photon beam is horizontal linearly polarized and perpendicular to our GeSe sample.

Electronic band structure calculation. All first-principles pseudopotential calculations for the band structure in the present work were performed, by using the projector augmented wave pseudopotentials²⁸ implemented in the Vienna ab initio Simulation Package²⁹. The Perdew–Burke–Ernzerhof approximation³⁰ was used to describe the exchange and correlation functional. The cutoff energy for the plane-wave basis and Monkhorst-Pack k -point mesh were set to 500 eV and $7 \times 6 \times 3$, respectively. To achieve the optimization of structure, the energy convergence threshold was set to 1×10^{-5} eV and the forces on each atom was set < 0.01 eV/Å. The van der Waals interactions were considered in all calculations based on the DFT-D3 Grimme method^{31,32}. The space group of GeSe is Pnma , $a = 3.87569$ Å, $b = 4.44484$ Å, and $c = 10.94380$ Å. The primitive cell contains four Ge and four Se atoms. The Ge ions are at positions of (0.2499a, 0.3826b, 0.1210c), (0.7501a, 0.6174b, 0.8790c), (0.7500a, 0.8826b, 0.3790c), (0.2501a, 0.1174b, 0.6210c), and the Se ions are at positions of (0.2500a, 0.4964b, 0.3538c), (0.7500a, 0.5036b, 0.6462c), (0.7500a, 0.9963b, 0.1462c), and (0.2500a, 0.0037b, 0.8538c).

XANES simulation. Simulations of the x-ray absorption near-edge spectrum at the Ge and Se *K*-edges were carried out with the finite difference method near-edge structure code³³. The calculations were performed using self-consistent non-muffin-tin potentials in an atomic cluster of 7 Å radius. Both dipolar and quadrupolar

contributions to the XANES cross section were taken into account. To compare to the experimental data, the computed spectra were convolved by a Lorentzian profile of full-width at half-maximum of 1.1 and 0.7 eV for Ge and Se, respectively.

Data availability

All data needed to evaluate the conclusions are present in the paper. Additional data related to this paper are available from the corresponding author upon reasonable request.

Received: 15 October 2020; Accepted: 14 May 2021;

Published online: 16 June 2021

References

- Nagai, M., Shimano, R. & Kuwata-Gonokami, M. Electron-hole droplet formation in direct-gap semiconductors observed by mid-infrared pump-probe spectroscopy. *Phys. Rev. Lett.* **86**, 5795 (2001).
- Heiplern, T. et al. Determination of hot carrier energy distributions from inversion of ultrafast pump-probe reflectivity measurements. *Nat. Commun.* **9**, 1853 (2018).
- Man, M. K. L. et al. Imaging the motion of electrons across semiconductor heterostructures. *Nat. Nanotechnol.* **12**, 36–40 (2017).
- Chen, Z. et al. Ultrafast dynamics of hot carriers in a quasi-two-dimensional electron gas on InSe. *Proc. Natl Acad. Sci. USA* **117**, 21962–21967 (2020).
- Chen, Z. et al. Band gap renormalization, carrier multiplication, and stark broadening in photoexcited black phosphorus. *Nano Lett.* **19**, 488–493 (2018).
- Brühwiler, P. A., Karis, O. & Märtensson, N. Charge-transfer dynamics studied using resonant core spectroscopies. *Rev. Mod. Phys.* **74**, 703 (2002).
- Garcia-Basabe, Y. et al. Ultrafast charge transfer dynamics pathways in two-dimensional MoS₂-graphene heterostructures: a core-hole clock approach. *Phys. Chem. Chem. Phys.* **19**, 29954–29962 (2017).
- Föhlisch, A. et al. Direct observation of electron dynamics in the attosecond domain. *Nature* **436**, 373–376 (2005).
- Garcia-Basabe, Y. et al. Species selective charge transfer dynamics in a P3HT/MoS₂ van der Waals heterojunction: fluorescence lifetime microscopy and core hole clock spectroscopy approaches. *Phys. Chem. Chem. Phys.* **21**, 23521–23532 (2019).
- Kühn, D. et al. Directional sub-femtosecond charge transfer dynamics and the dimensionality of 1T-TaS₂. *Sci. Rep.* **9**, 488 (2019).
- Johansson, F. O. L. et al. Tailoring ultra-fast charge transfer in MoS₂. *Phys. Chem. Chem. Phys.* **22**, 10335–10342 (2020).
- Eads, C. N., Bandak, D., Neupane, M. R., Nordlund, D. & Monti, O. L. A. Anisotropic attosecond charge carrier dynamics and layer decoupling in quasi-2D layered SnS₂. *Nat. Commun.* **8**, 1369 (2017).
- Johansson, F. O. L., Chen, X., Eriksson, O., Sanyal, B. & Lindblad, A. Interlayer charge transfer in tin disulphide: orbital anisotropy and temporal aspects. *Phys. Rev. B* **102**, 035165 (2020).
- Xue, D.-J. et al. GeSe thin-film solar cells fabricated by self-regulated rapid thermal sublimation. *J. Am. Chem. Soc.* **139**, 958–965 (2017).
- Shi, G. & Kioupakis, E. Anisotropic spin transport and strong visible-light absorbance in few-layer SnSe and GeSe. *Nano Lett.* **15**, 6926–6931 (2015).
- Zhao, H. et al. Band structure and photoelectric characterization of GeSe monolayers. *Adv. Funct. Mater.* **28**, 1704855 (2017).
- Wang, X. et al. Short-wave near infrared linear dichroism of two-dimensional germanium selenide. *J. Am. Chem. Soc.* **139**, 14976–14982 (2017).
- Xin, Y. et al. Polarization-sensitive self-powered type-II GeSe/MoS₂ van der Waals heterojunction photodetector. *ACS Appl. Mater. Interfaces* **12**, 15406–15413 (2020).
- Kennes, D. M., Xian, L., Claasen, M. & Rubio, A. One-dimensional flat bands in twisted bilayer germanium selenide. *Nat. Commun.* **11**, 1124 (2020).
- Xue, D.-J. et al. Anisotropic photoresponse properties of single micrometer-sized GeSe nanosheet. *Adv. Mater.* **24**, 4528–4533 (2012).
- Zhou, X. et al. Highly anisotropic GeSe nanosheets for phototransistors with ultrahigh photoresponsivity. *Adv. Sci.* **5**, 1800478 (2018).
- Zhao, L. et al. Ultrahigh power factor and thermoelectric performance in hole-doped single-crystal SnSe. *Science* **351**, 141–144 (2016).
- Brouder, C. Interlayer charge transfer in tin disulphide: orbital anisotropy and temporal aspects. *J. Phys. Condens. Matter* **2**, 701 (1990).
- Chen, Z. et al. Ultrafast electron dynamics reveal the high potential of InSe for hot-carrier optoelectronics. *Phys. Rev. B* **97**, 241201 (2018).
- Liu, S. et al. Alloy engineered germanium monochalcogenide with tunable bandgap for broadband optoelectrical applications. *Phys. Rev. Mater.* **4**, 074012 (2020).
- Rueff, J. P., Rault, J. E., Ablett, J. M., Utsumi, Y. & Céolin, D. HAXPES for materials science at the GALAXIES beamline. *Synchrotron Radiat. N.* **31**, 4–9 (2018).
- Rueff, J. P. The GALAXIES beamline at the SOLEIL synchrotron: inelastic X-ray scattering and photoelectron spectroscopy in the hard X-ray range. *J. Synchrotron Rad.* **22**, 175–179 (2015).
- Kresse, G. & J., D. From ultrasoft pseudopotentials to the projector augmented-wave method. *Phys. Rev. B* **3**, 1758–1775 (1999).
- Kresse, G. & J., F. Efficiency of ab-initio total energy calculations for metals and semiconductors using a plane-wave basis set. *Comp. Mater. Sci.* **1**, 15–50 (1996).
- Perdew, J. P., Burke, K. & Ernzerhof, M. Generalized gradient approximation made simple. *Phys. Rev. Lett.* **18**, 3865 (1996).
- Grimme, S., Antony, J., Ehrlich, S. & Krieg, H. A consistent and accurate ab-initio parametrization of density functional dispersion correction (DFT-D) for the 94 elements H-Pu. *J. Chem. Phys.* **132**, 154104 (2010).
- Grimme, S., Ehrlich, S. & Goerigk, L. Effect of the damping function in dispersion corrected density functional theory. *J. Comput. Chem.* **32**, 1456–1465 (2011).
- Bunau, O. & Joly, Y. Self-consistent aspects of x-ray absorption calculations. *J. Phys. Condens. Matter* **21**, 345501 (2009).

Acknowledgements

We thank DIM-Oximore and the Ecole polytechnique for funding under the project “ECO-GAN”. This work was supported by the EU/FP7 under the contract Go Fast (280555) and by “Investissement d’Avenir” Labex PALM (ANR-10-LABX-0039-PALM). We thank Synchrotron SOLEIL for provision of beamtime (proposal number 20181832).

Author contributions

Z.C., E.P., L.P., M.M., and J.-P.R. developed the project. Z.C. and J.-P.R. conducted the experiments and analyzed the data. GeSe band structure calculation was carried out by H.Q., and GeSe single crystal was grown by H.Z. and C.G., under the supervision of Y.C. Simulations of XANES was performed by J.-P.R. The manuscript was written by Z.C. and J.-P.R. All authors discussed the results and commented on the manuscript.

Competing interests

The authors declare no competing interests.

Additional information

Supplementary information The online version contains supplementary material available at <https://doi.org/10.1038/s42005-021-00635-y>.

Correspondence and requests for materials should be addressed to Z.C., Y.C. or J.-P.R.

Peer review information *Communications Physics* thanks the anonymous reviewers for their contribution to the peer review of this work.

Reprints and permission information is available at <http://www.nature.com/reprints>

Publisher’s note Springer Nature remains neutral with regard to jurisdictional claims in published maps and institutional affiliations.



Open Access This article is licensed under a Creative Commons Attribution 4.0 International License, which permits use, sharing, adaptation, distribution and reproduction in any medium or format, as long as you give appropriate credit to the original author(s) and the source, provide a link to the Creative Commons license, and indicate if changes were made. The images or other third party material in this article are included in the article’s Creative Commons license, unless indicated otherwise in a credit line to the material. If material is not included in the article’s Creative Commons license and your intended use is not permitted by statutory regulation or exceeds the permitted use, you will need to obtain permission directly from the copyright holder. To view a copy of this license, visit <http://creativecommons.org/licenses/by/4.0/>.

© The Author(s) 2021